

Review

# A Comprehensive Review of Layered Double Hydroxide-Based Carbon Composites as an Environmental Multifunctional Material for Wastewater Treatment

Yongxiang Huang <sup>1,2</sup>, Chongmin Liu <sup>1,2,3,\*</sup>, Saeed Rad <sup>1,2,3</sup> , Huijun He <sup>1,2,3</sup> and Litang Qin <sup>1,2,3</sup>

- <sup>1</sup> College of Environmental Science and Engineering, Guilin University of Technology, Guilin 541004, China; 19167547675@163.com (Y.H.); saeedrad1979@gmail.com (S.R.); hehj@glut.edu.cn (H.H.); qinsar@glut.edu.cn (L.Q.)
- <sup>2</sup> Guangxi Key Laboratory of Theory & Technology for Environmental Pollution Control, Guilin University of Technology, Guilin 541004, China
- <sup>3</sup> Collaborative Innovation Center for Water Pollution Control and Water Safety in Karst Area, Guilin University of Technology, Guilin 541004, China
- \* Correspondence: chongmin@glut.edu.cn

**Abstract:** As is well known, hydrotalcite-like compounds, such as layered-double-hydroxide (LDH) materials, have shown great potential applications in many fields owing to their unique characteristics, including a higher anion exchange capacity, a structure memory effect, low costs, and remarkable recyclability. While the lower surface area and leaching of metal ions from LDH composites reduce the process efficiency of the catalyst, combining LDH materials with other materials can improve the surface properties of the composites and enhance the catalytic performance. Among organic compounds, carbon materials can be used as synergistic materials to overcome the defects of LDHs and provide better performance for environmental functional materials, including adsorption materials, electrode materials, photocatalytic materials, and separation materials. Therefore, this article comprehensively reviews recent works on the preparation and application of layered double-hydroxide-based carbon (LDH-C) composites as synergistic materials in the field of environmental remediation. In addition, their corresponding mechanisms are discussed in depth. Finally, some perspectives are proposed for further research directions on exploring efficient and low-cost clay composite materials.

**Keywords:** adsorption; carbon; catalysis; LDH; LDH-C materials; removal mechanism



**Citation:** Huang, Y.; Liu, C.; Rad, S.; He, H.; Qin, L. A Comprehensive Review of Layered Double Hydroxide-Based Carbon Composites as an Environmental Multifunctional Material for Wastewater Treatment. *Processes* **2022**, *10*, 617. <https://doi.org/10.3390/pr10040617>

Academic Editors: Krzysztof Talaśka, Szymon Wojciechowski and Antoine Ferreira

Received: 19 February 2022

Accepted: 15 March 2022

Published: 22 March 2022

**Publisher's Note:** MDPI stays neutral with regard to jurisdictional claims in published maps and institutional affiliations.



**Copyright:** © 2022 by the authors. Licensee MDPI, Basel, Switzerland. This article is an open access article distributed under the terms and conditions of the Creative Commons Attribution (CC BY) license (<https://creativecommons.org/licenses/by/4.0/>).

## 1. Introduction

In recent years, a huge number of pollutants have been entering the environment through direct or indirect ways, causing environmental pollution and ultimately endangering the health of organisms. The direct or indirect intake of heavy metals in excess quantities through the food chain or contaminated water adversely affects the nervous and reproductive systems, damages vital organs, and causes several diseases, including Alzheimer's and Parkinson's [1]. In addition, several emerging pollutants, such as pharmaceuticals, personal care products (PCPs), veterinary products, food additives, and endocrine-disrupting chemicals (EDCs), have become a major environmental hazard due to their toxic effect (phytotoxicity and genotoxicity) on human and wildlife endocrine systems and fertility [2]. Therefore, developing novel and efficient environmental functional materials has attracted widespread attention. Among various materials, the layered double hydroxide (LDH) has been considered a potential material for environmental remediation because of its characteristics related to a controllable electronic structure, morphology, anion exchangeability, structure memory effect, low costs, and remarkable recyclability. Moreover, based on its excellent properties, it can as well serve as an ideal base material.

Many studies confirm that LDH-based materials have been widely applied for environmental remediation as functional materials for the removal of metalloids, heavy metals,

and organic pollutants. Huang et al. [3] prepared Fe<sup>2+</sup>-NiFe LDH to remove Cr(VI) oxygen anions, in which after five regeneration cycles, Fe<sup>2+</sup>-NiFe LDH still showed high Cr(VI) removal efficiency (>93%). Huo et al. [4] prepared Zn-Al and Mg-Al LDHs for removing a new type of persistent organic environmental pollutant (perfluorooctanoic acid), where the removal rate was higher than 98% after three cycles. However, the application and development of LDH materials are still limited by their wide bandgap, rapid photoelectron-hole recombination process, dense accumulation, and high leaching rate in the reaction process. Therefore, the recombination of LDHs with other semiconductor materials, such as carbon materials [5], to form heterogeneous structures is an effective way to improve their adsorption performance and catalytic activity. Carbon materials have many advantages, such as a wide range of sources, excellent pore structures, multiple active sites, and stable surface charge. Combined with LDHs, carbon materials can effectively reduce the agglomeration of LDHs during their nucleation process. In addition, they can compensate for the poor electrical conductivity of LDHs. Furthermore, LDHs can provide a template for carbon materials. Therefore, combining a carbon material with an LDH into a composite material with a novel structure and advanced surface properties is of practical importance.

A few review articles about LDHs have been published. For example, Mochane et al. [6] reviewed the morphology, thermal stability, and combustion performance of layered double-hydroxide/polymer nanocomposites. It was reported that LDHs are excellent alternatives for nanofillers in terms of flame retardancy improvement and barrier properties of polymer matrices. However, none of the previous works have discussed the application of LDH-C materials for adsorption and catalysis. To further explore the recent advances in the research works on LDH-based carbon composites in the field of adsorption and catalysis, this article reviews the synthesis of LDHs and LDH-based materials and their mechanisms and roles in the removal of non-metals, heavy metals, and new organic pollutants. Finally, the related perspectives and potential future advancements of LDH-based carbon materials are proposed in various fields.

## 2. Overview of LDHs and LDH-Based Composites

Layered double hydroxides (LDHs), commonly known as anionic clay, hydrotalcite, or hydrotalcite like, are one of the most widely studied nanomaterials [7]. They can be used as high-performance catalytic materials [8], adsorption materials [9], barrier materials [10], biomaterials [11], and separation materials [12] because of their characteristics in terms of interlayer anion exchange [13], acid base [14], memory effect [15], good catalytic performance [16], and thermal stability [17]. Moreover, an LDH can transform into a layered double oxide (LDO) at the temperature of 450–600 °C. Usually, an LDO is more stable than an LDH because of its large specific surface area, strong photosensitive catalytic activity, adjustable chemical composition, controllability of grain size and distribution, and unique memory effect [18–21]. In addition, LDOs are good options as carriers of redox catalysts or catalytic materials, attracting more and more attention as support materials in the field of catalysts. The composition, structure, properties, preparation methods, and applications of LDH-based carbon composites are summarized as follows.

### 2.1. General Structure and Properties of LDHs and Their Composites

#### 2.1.1. Composition, Characteristics, and Preparation of LDHs

The spatial structure of an LDH is shown in Figure 1. The typical molecular formula is  $(M_{1-x}M_x(OH)_2)^{x+}(A_{x/n})^{n-} \cdot mH_2O$ , where M<sup>2+</sup> and M<sup>3+</sup> represent the divalent and trivalent metal ions. The main layer structure is formed by the hydroxyl octahedrons of M<sup>2+</sup> and M<sup>3+</sup>, with anions interspersed between the main layer structures. The value of x refers to the charge density of the laminate, which is the molar ratio of M<sup>3+</sup>/(M<sup>2+</sup>+M<sup>3+</sup>). It is generally believed that a single-phase LDH can be obtained within x between 0.17~0.33 [22]. The principal characteristics of LDHs are determined by the type and molar ratio of the metal elements of the laminate, the type and quantity of interlayer particles, and the stacking form of laminates [23]. The divalent and trivalent metal cations used in the

synthesis of LDHs could be  $Mg^{2+}$ ,  $Mn^{2+}$ ,  $Fe^{2+}$ ,  $Co^{2+}$ ,  $Ni^{2+}$ ,  $Zn^{2+}$ , and  $Al^{3+}$ ,  $Mo^{3+}$ ,  $Fe^{3+}$ ,  $Co^{3+}$ ,  $Cr^{3+}$ ,  $Ga^{3+}$ , etc. [24].

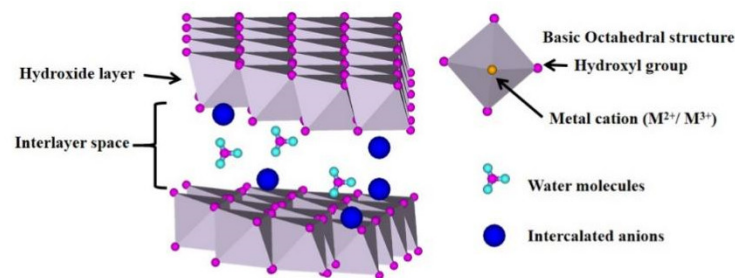


**Figure 1.** Schematic diagram of LDH spatial structure.

Currently, according to preparation processes, the synthesis methods of LDH include the salt-alkali preparation method (co-precipitation method) [25], microwave radiation synthesis [26], the ion exchange method [27], the in situ synthesis method [28], etc. The grain size and distribution of an LDH can be effectively controlled across a wide range by different preparation techniques. The size of LDH laminates prepared by the co-precipitation method is tens of nanometers, with small and uniformly distributed particles [29]. LDHs become layered by the urea synthesis method, and their particle sizes range from a few micrometers to 10  $\mu m$ . The structure of LDH is mainly related to the reaction time, the concentration of metal ions, and alkaline substances in the solution [30]. Among the above preparation methods, the hydrothermal synthesis of LDH has a complete crystal structure, high crystallinity, and uniform particles but experimental conditions are performed under high temperature, high pressure, and high power [31]. Currently, urea hydrolysis and hydrothermal synthesis techniques are used most frequently among the methods applied for LDH preparation.

### 2.1.2. The Characteristics of Carbon Materials and Preparation of LDH–Carbon Composites

Due to the outstanding advantages of carbon materials, such as rich types, wide sources, good pore structure, countless active sites, and stable surface charges, researchers adopt different modification methods for various carbon materials to improve the defects of carbon materials and their applications and performance. Commonly used carbon materials include active carbon (AC), active carbon fibers (ACFs), bio-carbon (BC), carbon nanotubes (CNTs), fullerene ( $C_{60}$ ), graphene (GO), etc. At present, the known carbon materials used with LDHs to create composites mainly include biochar, fullerene, carbon nanotubes, and graphene.

#### (1) Biochar (BC)

Many studies have shown that biochar is suitable for immobilizing organic pollutants in soil and water due to its high aromaticity, abundant surface functional groups, microporous surface, and high specific surface area [32]. The key mechanisms in biochar immobilization of organic pollutants include the distribution of non-carbonized components, pore filling, electrostatic attraction,  $\pi$ - $\pi$  electron donor-acceptor interaction, and hydrophobic effect [33]. The surface polarity and aromaticity of biochar are considered to be the most important characteristics affecting the affinity of organic pollutants, which are controlled by kinds of raw materials, pyrolysis conditions, and modification methods [34]. Known modification methods for biochar include magnetic modification, mineral modification, acid modification, alkali modification, oxidant modification, photocatalyst modification, electrochemical modification, nanocarbon material modification, and methanol modification [32]. Among them, the biochar obtained after alkali treatment is conducive to the adsorption of organic matter.

## (2) Fullerene (C<sub>60</sub>)

Fullerene (C<sub>60</sub>) is a hollow molecule composed entirely of carbon. Fullerene and its derivatives have many excellent properties, such as superconductivity, semiconductor, and strong magnetism. They have potential applications in the fields of light, electricity, and magnetism.

## (3) Carbon nanotubes (CNTs)

Carbon nanotubes (CNTs) are hexagonal network structures composed of sp<sup>2</sup> hybrid carbon atoms, which are completely bonded with adjacent carbon atoms. The network structure is bent according to a certain helix angle to form a seamless one-dimensional space topology. Because of large specific surface areas, excellent electron storage capacity, and electron transport capacity, CNTs can provide abundant adsorption sites for catalytic reactions to promote the separation of photogenerated electrons from vacancies. Therefore, CNTs are suitable for supercapacitors and catalysis.

## (4) Graphene (GN/RGO)

Graphene (GN) is a two-dimensional carbon material with an atom-thick carbon sheet formed by sp<sup>2</sup> hybridization of carbon atoms. Due to its unique structure, GN has high conductivity, high stability, high thermal conductivity, and excellent mechanical strength. It is the thinnest, hardest, and most conductive material known so far. It is mainly used in supercapacitors. Graphene oxide contains a large number of oxygen-containing functional groups after peroxidation treatment, which can increase its hydrophilicity and ion exchange capacity. Therefore, GO can be used to adsorb heavy metal ions. The good conductivity of carbon materials can promote contact between active sites and electrolytes, which can accelerate ion/electron transfer.

The combination of a layered double hydroxide and a carbon material will increase the surface area and enrich the oxidizing functional groups, which can significantly improve the surface performance, adsorption capacity, and catalytic activity of the catalyst. The LDH–carbon material composites have exceptional physical and chemical properties. The methods for preparing the composites of carbon material are as follows:

- (1) Direct mixing: The positively charged surface of LDHs and the negatively charged surface of carbon nanomaterials are assembled into LDH–carbon material composites through electrostatic force action. Liu et al. [35] used benzoic acid to intercalate an LDH, mixed the resulting material with a xylene solution containing C<sub>60</sub>, and stirred the mixture ultrasonically for 48 h at 70 °C to obtain a C<sub>60</sub>–LDH composite with C<sub>60</sub>-intercalated LDH. These C<sub>60</sub>–LDH materials can be obtained on a large scale by this simple, convenient, and low-cost preparation process. However, this method is not suitable to obtain a desired ideal structure because of the complicated interaction between carbon and the LDH.
- (2) Self-assembly: Relying on the force between molecules or ions, the combination of materials is changed from a disordered combination to an orderly combination. This method can control the material's structure with required functions. Lestari et al. [36] co-precipitated ZnTi LDH in a homogeneous solution and then vigorously stirred Ag and C<sub>3</sub>N<sub>4</sub> powder with the LDH in ultrapure water to complete the self-assembly reaction. The prepared material was combined by electrostatic force. Although the bonding process can be controlled, the overall material is unstable and requires further processing.
- (3) Growth in situ: A carbon material can be grown with an LDH as a substrate, or an LDH can also be grown using a carbon material as the substrate. In the preparation process, the carbon material adsorbs cations on its surface and these cations co-precipitate on the surface of the carbon material to form a new LDH. Similarly, the material can enter the inner layer of the LDH or use the LDH as a catalytic precursor to grow the carbon material. Li et al. [37] mixed the alkali solution of graphite oxide and the solution of Ni(NO<sub>3</sub>)<sub>2</sub> and Al(NO<sub>3</sub>)<sub>3</sub> to prepare graphene–LDH composites. This method mainly

relies on the attraction of negatively charged carbon materials to positively charged cations of the LDH precursor solution. The size of the LDH prepared by this method is affected by the nanometer size of the carrier carbon material.

### 3. Research on the Application of LDH–C Materials

#### *Application of LDH–C Composite as Environmental Remediation Materials*

LDH–C is a potential environmental remediation material that has been used for removing various pollutants, such as heavy metals, inorganic anions (such as nitrates and phosphates), and organic pollutants. This review summarizes some of the literature in recent years about the application of LDH–C materials in adsorption, photocatalysis, and electrocatalysis, as shown in Table 1.

**Table 1.** Application of LDH–C materials in water pollution.

Applications	Composites	Carbon Material	Synthetic Methods	Pollutants	Efficiency	References
Adsorption	MAC/MgAl LDO	Magnetite-activated carbon	Co-precipitation	Iodide	86%	[38]
	CuAl/CF LDH	Carbon fiber	One-pot hydrothermal technology	Phosphates	100 mg·g <sup>-1</sup>	[39]
	NiZnFe LDH/BC	Date palm biochar	Co-precipitation	RB5 dye	90%	[40]
	MnAl LDH/BC	Oil tea camellia shells	Hydrothermal synthesis	Cu	74.07 mg·g <sup>-1</sup>	[41]
	NiFe CO <sub>3</sub> -LDH/NGO	NGO	Probe-sonication-mediated process	Cadmium and lead	971 mg·g <sup>-1</sup> ; 986 mg·g <sup>-1</sup>	[42]
	ZnAl LDH/BC	Sludge biochar	Co-precipitation	BTA and Pb(II)	239.6 mg·g <sup>-1</sup> ; 226.1 mg·g <sup>-1</sup>	[43]
Photocatalysis	CoAl LDH/OCN	OCN	In situ hydrothermal method	Methyl orange	0.09568 min <sup>-1</sup>	[44]
	C <sub>60</sub> @ZnAlTi LDH	C <sub>60</sub>	Urea hydrolysis	Bisphenol A	80%	[45]
	ZnAl LDH/g-C <sub>3</sub> N <sub>4</sub> /CuONP	g-C <sub>3</sub> N <sub>4</sub>	Co-precipitation	Phenol	94%	[46]
	CoAl LDH/CN/RGO	CN/RGO	One-step hydrothermal method	Congo red and tetracycline	80%; 90%	[47]
Adsorption and photocatalysis	MgAl CLDH/g-C <sub>3</sub> N <sub>4</sub>	g-C <sub>3</sub> N <sub>4</sub>	Co-precipitation	Congo red	99.7%	[48]
	MgZnAl LDH/g-C <sub>3</sub> N <sub>4</sub>	g-C <sub>3</sub> N <sub>4</sub>	Green template method	Tetracycline	96.95%	[49]
	MnFe LDO/BC	Palm-seed-based biochar	Facile co-precipitation followed by calcination	Tetracycline	98%	[50]
Electrocatalysis	NiFe LDH/CNT	CNT	Urea hydrolysis	Ethanol	30.5 mA·cm <sup>-2</sup>	[51]
	FQD/CoNi LDH/NF	FQD	Self-assembly process	Water and urea	10 mA·cm <sup>-2</sup>	[52]
	NiCoCe LDH/CNT	CNT	Solvothermal self-assembly process	Water	10 mA·cm <sup>-2</sup>	[53]

As presented in Table 1, LDH–C exhibited efficient adsorption of organic and inorganic pollution. Wang et al. [38] used applewood waste as a raw material of biomass to prepare biochar (AB) through pyrolysis and CO<sub>2</sub> activation and loaded MgAl LDHs to prepare a new carbon adsorbent (AMB). The adsorption results showed that the average adsorption capacity of AMB for NO<sub>3</sub><sup>-</sup> was 7.43 times higher than that of AB and the average removal rate of NO<sub>3</sub><sup>-</sup> increased from 13% to 83%. Wang et al. [41] prepared an oil-tea camellia shell (OCS) biochar/MnAl–LDH material by hydrothermal synthesis to remove Cu(II) from the aqueous solution, with a maximum adsorption capacity of 74.07 mg·g<sup>-1</sup>. LDHs combined with different carbons demonstrated efficient photocatalysis as well. Kumar et al. [54] prepared nanoscale ZrRGO/CuFe–LDH composites by the co-precipitation method for enhanced photocatalytic degradation of dye contaminant. The experimental results showed that the material obtained an excellent energy band in the range of 1.74 to 2.0 eV. Under visible light, the photodegradation rate of methylene blue reached 95.2%, and the total organic matter removal rate reached 92%. Motlagh et al. [55] synthesized ZnFe–Cl–LDH/GO and ZnFe–SO<sub>4</sub><sup>2-</sup>–LDH/GO photocatalysts, which were used to decompose

ofloxacin (OFX) under visible light irradiation, and the degradation efficiency was 71.19% after 150 min of irradiation.

What is more, the removal rate was higher than 96% in the process of the adsorption and photocatalytic synergistic action. Wang et al. [48] reported a novel hierarchical architecture composed of MgAl-LDH nanosheets and g-C<sub>3</sub>N<sub>4</sub>, which showed an effective adsorption-photocatalytic synergistic effect for Congo red removal under simulated sunlight exposure. Bin et al. [56] prepared a magnetic recoverable g-C<sub>3</sub>N<sub>4</sub>/CoFe-LDH catalyst for hexavalent chromium removal, demonstrating that the nanocomposite material can adsorb 60% of hexavalent chromium (50 mg·L<sup>-1</sup>) within 10 min under visible light irradiation and the removal rate of hexavalent chromium (50 mg·L<sup>-1</sup>) can reach 100% within 90 min under the synergistic effect of adsorption and photocatalysis. The excellent adsorption and photocatalytic properties can be attributed to stronger stability, more surface-active sites, and functional groups of the LDH-based carbon composites. Therefore, LDH-C materials are effective adsorbents and catalysts to remove inorganic and organic pollutants. The excellent performance is attributed to the properties of the composite, which solve the problem of dense accumulation and the high leaching rate of LDH. On the one hand, the part of carbon is used for preventing LDH agglomeration, and on the other hand, the part of LDH is mainly responsible for the adsorption and degradation of pollutants. LDH-C also exhibits excellent performance in the electrocatalysis of ethanol, water, and urea.

#### 4. Mechanism Analysis of LDH-C as Various Remediation Materials

##### 4.1. Mechanism Analysis of LDH-C as Adsorption Materials

###### 4.1.1. Adsorption Mechanism of Non-Metal Elements

Inorganic anions mainly include phosphate, nitrate, ammonium, and arsenic. Because nitrogen, phosphorus, and arsenic belong to the same main group, their properties have many similarities. Zheng et al. [57] prepared a synthetic material of LDH-modified biochar combined with sodium alginate to improve the removal of nitrogen and phosphorus in the bioreactor. The results showed that under the optimum conditions, the removal rates of phosphate and nitrate reached 86.11% and 95.32%, respectively. Adsorption kinetics and isothermal adsorption fit well with the pseudo-second-order and Langmuir isotherm models, respectively, indicating that the adsorption process is mainly controlled by chemical adsorption (such as electron exchange between adsorbate and adsorbent). Hu et al. [39] also carried out similar experimental research, successfully synthesized a hierarchical CuAl/biomass carbon fiber layered double hydroxide, enhanced oxide, and applied it to the adsorption of phosphate in simulated wastewater. The adsorption of phosphate reached equilibrium in about 50 min, and the removal rate reached 99.6%. FTIR and Raman spectroscopy (RS) analysis showed that anion exchange, electrostatic adsorption, and ligand exchange mainly occurred in the process of phosphate adsorption. The results also showed that the phosphate removal kinetics accorded with the pseudo-second-order model and the adsorption isotherm were in line with the Langmuir model. In addition, the regeneration potential and reuse experiments of waste adsorbent show that the composite has a high recovery capacity. Therefore, it can be considered that the prepared graded composite is an effective adsorbent for removing phosphate from wastewater.

Wang et al. [38] studied the adsorption characteristics and mechanism of NO<sub>3</sub><sup>-</sup> on Mg/Al-LDH composite apple biomass (AMB) by batch adsorption experiment, the adsorption model, and various characterization methods. The chemical modification of Mg/Al LDHs on the surface of AB causes electrostatic interaction, which makes AB positively charged, resulting in the electrostatic attraction of AMB to NO<sub>3</sub><sup>-</sup>, which is given by aromatic heterocyclic compounds. The electrons also form a stable structure with NO<sub>3</sub><sup>-</sup>, which enables NO<sub>3</sub><sup>-</sup> to fully penetrate the pores of AMB.

Therefore, the adsorption mechanism of non-metal elements mainly includes physical and chemical composite adsorption, including surface physical sorption, intraparticle diffusion, electrostatic adsorption, ion exchange, and metal-bonded bridges, as shown in Figure 2.

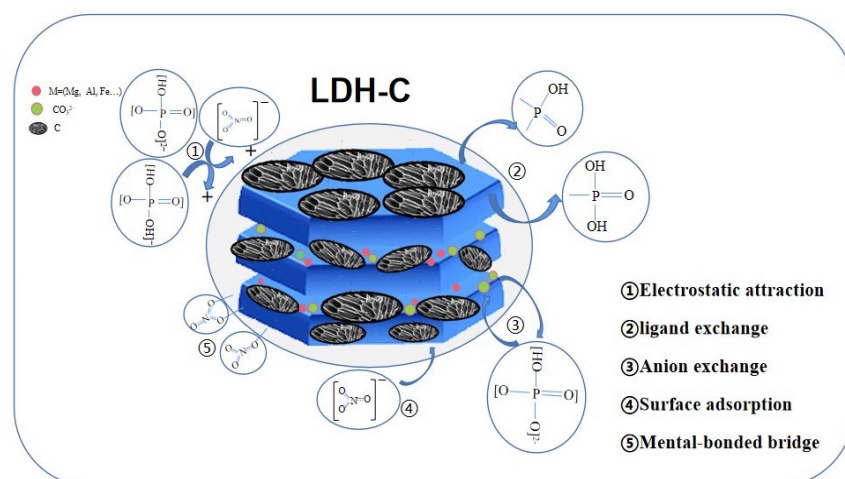


**Figure 2.** Adsorption mechanism of non-metal elements.

#### 4.1.2. Adsorption Mechanism of Heavy Metals

At present, the adsorption of heavy metals includes heavy metal cations, heavy metal anions, radionuclides, and so on. For instance, Lai et al. [58] produced carbon nanosheets in situ by hydrothermal and high-temperature carbonization methods to prepare organic LDHs for the adsorption of Cr(VI) and Cd(II). The experimental results show that samples prepared by the hydrothermal method are rich in carboxyl and sulfonic acid groups while the high-temperature carbonization products mainly contain hydroxyl and thiophenol/mercaptan. Due to the existence of thiophenol/mercaptan groups in LDH carbon, it can produce complexation so that the adsorption capacity of Cr(VI) and Cd(II) is 4.4 times and 6.7 times higher than that of the LDH, respectively. Therefore, high-temperature carbonization treatment is more conducive to producing a large specific surface area of the composite. The addition of carbon provides enough functional groups and active sites. The existence of an electrostatic adsorption mechanism also causes the secondary arrangement of interlayer anions, which can effectively promote the adsorption of heavy metals. In addition, Huang et al. [59] prepared MgAl-LDH/graphene nanocomposites (MGL) by the one-pot solvothermal method. The adsorption efficiency of MGL for Pb, Cu, and Cd in an aqueous solution was evaluated by a batch equilibrium experiment. Through XRD analysis, the XRD characteristic peak of CdCO<sub>3</sub> precipitation was found after Cd(II) adsorption. The XPS spectrum shows the generation of Cu(OH)<sub>2</sub> precipitation, which proves the adsorption of Cu<sup>2+</sup> and that the formation of hydroxide is related to the existence of functional groups such as carboxyl and hydroxyl. The above indicates that the adsorption mechanism is caused by the surface complexation of functional groups, the precipitation of a metal hydroxide or a metal-carbon oxide and the isomorphic replacement of Mg<sup>2+</sup>. Two-dimensional transition metal carbides are new two-dimensional structural materials. They are not only characterized by high specific surface area and high conductivity of graphene but also have the advantages of flexible components and controllable minimum nanolayer thickness. Feng et al. [9] synthesized alk-MXene-LDH composites by compounding MXene and LDH. The adsorbent has a unique layered structure and the saturated adsorption capacity of Ni<sup>2+</sup> is 222.72 mg·g<sup>-1</sup>. After the adsorption of Ni(II) ions, many tiny nanoparticles are adsorbed on the layered surface of alk-MXene-LDH. The existing forms of these nanoparticles are as follows: Ni(OH)<sub>2</sub>, NiO(OH), (Ni<sub>1-x</sub>Al<sub>x</sub>(OH)<sub>2</sub>)CO<sub>3x/2</sub>, and NiCO<sub>3</sub>. The removal path of Ni(II) ions in the aqueous phase is mainly chemical adsorption rather, not physical adsorption, which is manifested by precipitation and coordination complexation. Peng et al. [60] used phosphate-impregnated bamboo biochar composite MgAl-LDH (PBC@LDH) to study the radioactive element uranium. Since the adsorption capacity of biomass is weak and the radioactive element uranium can form highly stable uranyl phosphate compounds with phosphate, it is a suitable strategy for phosphate impregnation and activation of bamboo charcoal. The adsorption of U(VI)

is not only due to the high specific surface area of the composite material but also due to the fact that P–O, Mg–O–H, and –OH have strong complexation and co-precipitation effect on U(VI).

As shown in Figure 3, the adsorption mechanism of LDH composite carbon materials for heavy metals includes isomorphous substitution, electrostatic interaction, complexation, and surface precipitation. Although there are many studies on the adsorption of heavy metals, there are still some metal ions, such as  $\text{Hg}^{2+}$  and  $\text{Ag}^+$  removal mechanisms, that have not been explored clearly.

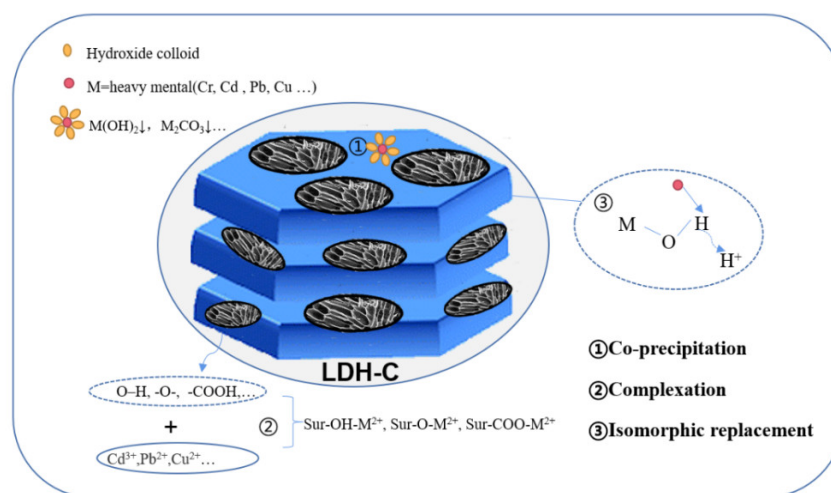


**Figure 3.** Adsorption mechanism of heavy metals.

#### 4.1.3. Adsorption Mechanism of Organic Pollutants

Organic pollutants are a class of complex substances that usually contain functional groups, such as benzene rings, hydroxyl groups, and amino groups. The main adsorption mechanisms of organic pollutants are electrostatic attraction, anion exchange, hydrogen bond, and  $\pi$ – $\pi$  interaction. Sun et al. [61] combined the biological template method and the hydrothermal method to synthesize a porous layered MgAl–LDH/CF (carbon fiber) composite material with good adsorption properties. Cotton is composed of long elastic fibers that cross each other to form a loose porous structure. The experimental results show that the maximum adsorption capacity of MgAl–LDH/CF for Congo red dye is  $271.00 \text{ mg}\cdot\text{g}^{-1}$ , which is significantly higher than that of MgAl LDH synthesized without the biological template method. After four adsorption–desorption cycles, MgAl LDH/CF still maintained 85.33% of the maximum adsorption capacity. Characterization analysis confirmed that the adsorption capacity of composite materials is closely related to porosity and surface area, both of which provide active sites for adsorption. Anion exchange and electrostatic adsorption are considered to be the main adsorption mechanisms.

Allou et al. [13] used the co-precipitation method to successfully deposit flake MgAl LDH on the surface of activated carbon. The hybrid nanocomposite material was used as a carrier for the antibiotic norfloxacin (NOR). Only when the pH is around 7.4 is norfloxacin completely dissolved and absorbed. Oxygen functional groups such as epoxy, carbonyl, hydroxyl, and carboxyl groups on the surface of biomass carbon are effective agents to increase the negative charge on the surface. According to the analysis of the diffraction peaks in the XRD pattern, the deposition occurs in the gap of the LDH, indicating that the positively charged LDH is supported on the negatively charged carbon surface. Sirajudheen et al. [62] prepared a ZnAl–LDH@C composite material to remove toxic Congo red (CR), Acid red 1 (AR1), and Reactive red 2 (RR2) dyes in water. He proposed possible adsorption mechanisms for dyes, including electrostatic attraction caused by the interaction between negatively charged dye molecules and positively charged adsorbents. During the reaction, the LDH and activated carbon provide hydrogen bonds, dye molecules act as hydrogen

bond acceptors, and dyes act as ligands to form surface complexation with the hydrated part of the LDH. There is also an ion exchange between the intercalated  $\text{CO}_3^{2-}$  in the composite material and the  $\text{SO}_3^{2-}$  in the azo dye.

In summary, the relatively developed pore structure, internal electrostatic interaction, van der Waals force,  $\pi$ - $\pi$  interaction, and other chemical bonding effects of the LDH, as well as the positive charge and alkalinity of the main laminate, and the exchangeability of interlayer anions, make this composite material a good alternative to be used as an adsorbent. Organic pollutants are adsorbed on the LDH composite through  $\pi$ - $\pi$  bonds, hydrophobic interactions and hydrogen bonds, surface complexation, precipitation, and isomorphous replacement, as shown in Figure 4.

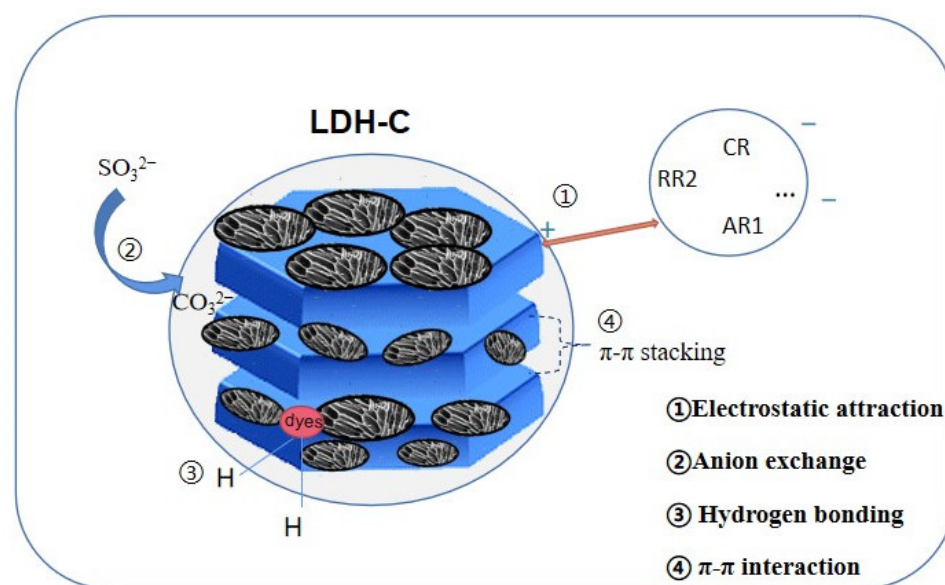


**Figure 4.** Adsorption mechanism of organic pollutants.

#### 4.2. Mechanism Analysis of LDH-C as Catalytic Materials

##### 4.2.1. Mechanism as Electrocatalytic Materials

Because the conductivity of an LDH can be improved when it forms a composite with carbon nanotubes, the composites can be used as electrode catalyst materials. A suitable electrocatalyst can reduce the overpotential and increase the reaction speed, thereby improving the energy conversion performance. Yang et al. [51] prepared a three-dimensional spherical composite of carbon nanotubes (CNTs) and layered double hydroxides (NiFe LDHs) by urea synthesis without using any surfactants or organic solvents. Ni(II) and Fe(III) ions are adsorbed on the surface of carbon nanotubes, and carbon nanotubes gather interwoven clusters to form a conductive network. In the presence of urea, the sequential hydrolysis and polycondensation of Fe(III) kinetics facilitate the precipitation of amorphous iron hydroxide. According to the electrochemical impedance spectroscopy (EIS) in the electrocatalytic test, compared with the NiFe-LDH powder sample, the NiFe-LDH-CNT composite material significantly enhances electrocatalytic activity (about 5 times), showing a smaller value of  $15.7 \Omega$  electron transfer resistance and increased long-term stability of ethanol oxidation. Furthermore, Dinari et al. [53] researched the electrocatalytic activity of the cerium-doped nickel-cobalt layered double hydroxide on carbon nanotube scaffolds for an oxygen evolution reaction (OER). LDH grows on carbon nanotubes to form a conductive network through which suitable conductivity for electron transfer can be achieved. The surface area of NiCoCe LDH/CNT doped with 10% Ce in the structure can reach  $52.63 \text{ m}^2 \cdot \text{g}^{-1}$ , which helps to reduce the blockage of LDH nanosheets, thereby increasing the surface area of the electrolyte that comes in contact with the catalyst. Compared with other proportions of catalysts, NiCoCe LDH (10% Ce) has a higher current density (current density is proportional to oxygen production), lower overpotential, and the highest

OER activity. The improvement of the OER activity of the electrocatalyst is attributed to the strong electron transport, lattice defects, special surface area, and large range of  $Ce^{3+}$  coordination number in the nanostructure. This research has achieved a breakthrough in the large-scale preparation of non-precious-metal-lanthanide-doped LDH nanocomposites.

Therefore, the electrocatalytic mechanism is shown in Figure 5 and can be summarized as follows: (1) The embedding of semiconductor materials with good conductivity  $-NH_2$ ,  $-OH$ , and  $-COOH$  groups can promote the charge transfer of a LDH; (2) the rough surface of the porous conductive substrate can not only increase the exposed edge of the LDH, generating more active sites, but also enhance the rapid release of gas precipitation; (3) in addition, to prevent additional resistance, the use of polymer binders during electrode preparation should be avoided when supporting the electrode.

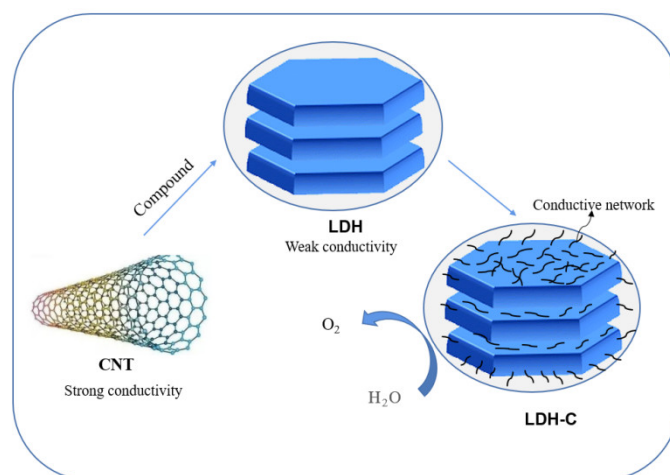
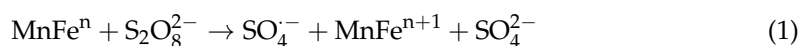


**Figure 5.** Mechanism as electrocatalytic materials.

#### 4.2.2. Mechanism as Photocatalytic Materials

Recently, research emphasis has been geared toward hydrotalcite-like materials that have layered structures (LDH) and can be used as photocatalysts. The LDH's calcination is an outstanding technique for the synthesis of uniformly dispersed mixed metal oxides (LDOs) with superior photocatalytic efficiency to traditional methods. Azalok et al. [50] used the co-precipitation–calcination process to successfully synthesize a highly efficient LDH-biological carbon hybrid catalyst for the removal of tetracycline pollution. This research highlights the powerful synergistic combination of an LDH and biochar. The mixed catalyst has a high specific surface area ( $524.8 \text{ m}^2 \cdot \text{g}^{-1}$ ) and a suitable pore size of 3.65 nm, which provides sufficient reaction sites in the bulk solution. The photodegradation mechanism of tetracycline (TC) is mainly induced by  $OH^\cdot$ , while  $SO_4^{\cdot-}$ ,  $h^+$ , and  $O_2^{\cdot-}$  also contribute partly to mineralization. Under optimized conditions, in the presence of oxidants ( $K_2S_2O_8$  and  $H_2O_2$ ), the degradation rate was significantly reduced. After three consecutive cycle tests, stable catalytic reuse activity was maintained.



MnFe LDO biochar exhibits sufficient transient photocurrent response ( $3.8 \mu\text{A} \cdot \text{cm}^{-2}$ ), which is higher than MnFe LDO ( $3.45 \mu\text{A} \cdot \text{cm}^{-2}$ ), indicating that the synergistic combination of biochar and MnFe LDO improves the separation rate and the stronger suppression of photogenerated hole–electron recombination improves the photocurrent response of the hybrid catalyst.

Ju et al. [45] used the urea method to prepare fullerene ( $C_{60}$ ) combined with ZnAlTi layered double hydroxide (ZnAlTi LDH) and photodegraded bisphenol A (BPA) under simulated visible light irradiation. The photoactivity of the ZnAlTi–LDO catalyst was enhanced by  $C_{60}@AgCl$ , which because of Ag-enhanced near field could boost the excitation of electron–hole pairs in ZnAlTi LDO. Therefore, using  $C_{60}$  as the carrier material can improve the stability of the silver-based photocatalyst. Photogenerated holes, superoxide radicals, hydroxyl radicals, and singlet oxygen (excited oxygen molecules) are supposed to be the cause of the photocatalytic degradation process. The addition of  $C_{60}$  semiconductors can promote the degradation and complete mineralization of various pollutants and can cause rapid light-induced charge separation during the electron transfer process and lead to relatively low charge recombination.

Wu et al. [44] constructed a 2D/2D heterostructure composed of oxygen-doped carbon nitride (OCN) and an ultra-thin layered double hydroxide (coalldh) by the in situ growth method and photocatalytic degradation of methyl orange (MO) dye under visible light conditions. A 2D/2D OCN/coal LDH with a flower structure has a high specific surface area, good mesoporous properties, and large pore volume, which is conducive to the exposure of active sites and the diffusion of pollutants and active radicals in the photocatalytic process. The positively charged ions in coal LDH are adsorbed on the surface of negatively charged OCN sheets through electrostatic force, resulting in strong coupling to form the internal electric field of the interface. Therefore, the high specific surface area, the strong electron coupling effect in the mesoporous heterostructure interface, visible light absorption performance, and the excellent photogenerated charge carrier separation ability of the new photocatalyst make the photocatalytic degradation efficiency of the hybrid catalyst dozens or even hundreds of times higher than that of pure OCN and a pure LDH. In addition, Jo et al. [47] used the LDH/CN/RGO ternary heterojunction system for the photocatalytic decomposition of Cr and TC pollutants. The significant 2D/2D/2D arrangement between LDH/CN/RGO promotes the interfacial charge transfer and hinders the direct recombination of photoinduced electron–hole pairs, which makes the degradation performance significant. In addition, LDH/CN/RGO ternary heterojunction shows obvious optical absorption in the visible region, which can produce more photoinduced carriers for the degradation reaction. The quenching free radical experiment also showed that  $O^{2-}$ ,  $H^+$ , and  $\cdot OH$  participated in the decomposition reaction, and the influence order was  $O^{2-} > H^+ > OH$ .

In conclusion, the application mechanism of LDH-combined carbon materials in photocatalysis is shown in Figure 6 and explained as follows: (1) In the photocatalysis process, the valence band is excited to produce holes and generate electron–hole pairs. The recombination degree of holes and electrons depends on the capture process of holes and electrons on the catalyst surface and the migration process of surface charges, which affects the quantum efficiency of photocatalysis [48,63]. The synergistic combination of carbon materials and the LDO is to gain the photocurrent effect of the hybrid catalyst by increasing the rate of charge separation and inhibiting photogenerated hole–electron pair recombination [50]. (2) Through free radical capture, determination of the active free radicals in the photocatalytic degradation reaction, such as photogenerated holes ( $h^+$ ), superoxide radicals ( $O^{2-}$ ), hydroxyl radicals ( $OH^-$ ), photogenerated electrons ( $e^-$ ), and single-line oxygen (excited oxygen molecules), has been considered an important factor in photocatalytic degradation [44]. (3) The high photocatalytic activity of the composite material is also due to the dispersion of the stripped carbon material on the LDH, and a massive energy transfer occurs in the charge carrier. The positively charged LDH adsorbs the negatively charged carbon material on the surface through electrostatic forces, which produces a coupling effect, forming a flower-like structure, which can constitute an interfacial electric field in an equilibrium state and further promote the formation of superoxide radicals [44]. All the above factors promote the enrichment of anionic pollutants around the carbon material, effectively shortening the diffusion distance and accelerating the degradation of contaminants [46].

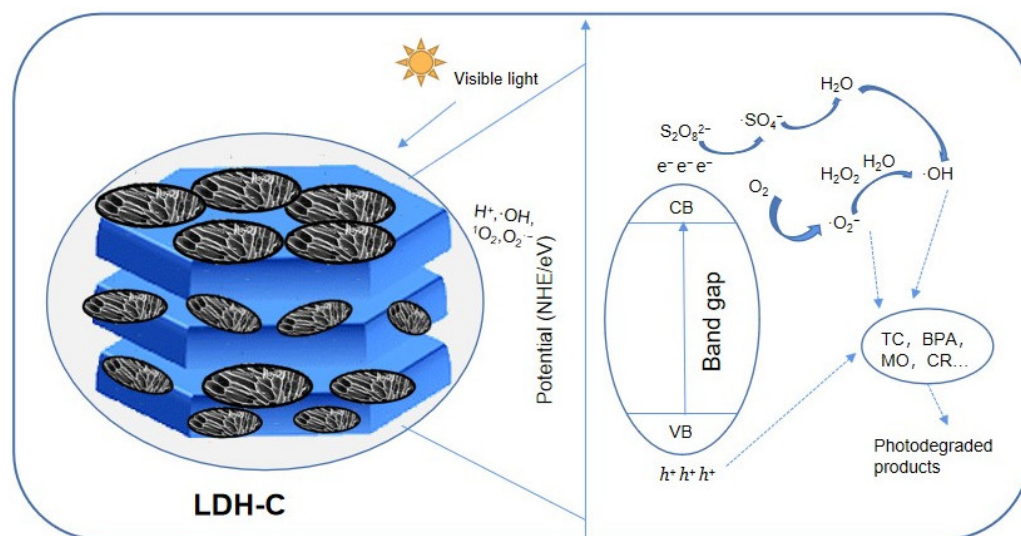


Figure 6. Mechanism as photocatalytic materials.

The photocatalytic mechanism based on an LDH photocatalyst has not yet been fully explained. Advanced characterization techniques, such as in situ electron spin resonance, in situ nuclear magnetic resonance, and in situ infrared spectroscopy, can be used later under reaction conditions to get a deeper mechanism [22]. Research can also be combined with theoretical models to design more reasonable photocatalytic LDH–carbon materials, optimize the material structure, predict active catalytic sites, and determine bandgap energy and location.

#### 4.2.3. Mechanism as Synergistic Materials for Adsorption and Photocatalysis

There are few studies on LDH–C materials with both adsorption and photocatalytic properties. Among carbon composite materials, the properties of graphite carbon and LDHs are more prominent. Liu et al. [64] synthesized ZnCr–LDH/N-doped graphite carbon (g-C<sub>3</sub>N<sub>4</sub>) composites by the co-precipitation method and hydrolyzed Congo red under visible light irradiation. The degradation of Congo red is divided into two steps. Firstly, the dye is adsorbed around the catalyst and inserted into the composite through an anion exchange, and then the photocatalytic reaction occurs under visible light irradiation. The 2D/2D nanostructured LDH is dispersed on g-C<sub>3</sub>N<sub>4</sub>-C(N), which increases the specific surface area of g-C<sub>3</sub>N<sub>4</sub>-C(N) to expose more adsorption sites and improve the adsorption performance of the composite material. In addition, g-C<sub>3</sub>N<sub>4</sub>-C(N) with the extended and delocalized  $\pi$ -conjugated system has certain conductivity, which is beneficial to the transport of electrons in ZnCr–LDH and contributes to reduce the recombination rate of electron–hole pairs, which can directly oxidize the organic pollutants in the solution. Hydroxyl radicals and superoxide radicals oxidize large molecules of dyes into small molecules, which are more conducive to adsorption, thereby improving photocatalytic performance. Yu et al. [49] successfully prepared a modified g-C<sub>3</sub>N<sub>4</sub>/MgZnAl-calcined layered double hydroxide (M-CN–cLDH) composite material by the template method, which was used to eliminate the typical tetracycline antibiotics in seawater, namely oxytetracycline (OTC), tetracycline (TC), chlortetracycline (CTC), and doxycycline (DXC). The results show that after 120 min of visible light irradiation, the synergistic removal rate of M-CN cLDH on OTC in seawater is 2.73 times higher than that of g-C<sub>3</sub>N<sub>4</sub>. In the continuous flow reaction process, M-CN cLDH also has good adsorption and photocatalytic degradation of OTC. The excellent adsorption capacity of M-CN cLDH is attributed to the open porous structure of cLDH, and its excellent photocatalytic degradation activity is attributed to the tightly bound heterostructure between the g-C<sub>3</sub>N<sub>4</sub> (CN) and cLDH bilayers.

The synergistic mechanism of adsorption and photocatalysis is summarized in Figure 7: (1) the LDH's super anion exchange capacity, large specific surface area, more adsorption

sites, and open porous structure promote the adsorption of pollutants, (2) the high conductivity of carbon materials accelerates the electron transport and reduces the recombination rate of electron–hole pairs to improve the photocatalytic efficiency, (3) the existence of hydroxyl radical and superoxide radical in the composites also accelerates the degradation of pollutants, and (4) the heterojunction between the LDH and carbon materials bilayer also enhances the photocatalytic activity.

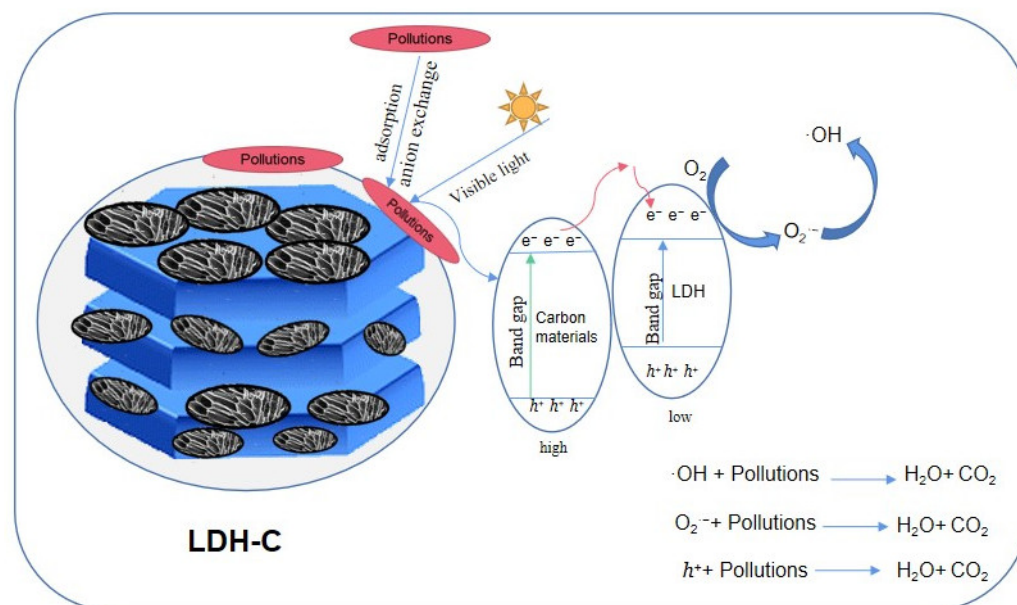


**Figure 7.** Mechanism as synergistic materials for adsorption and photocatalysis.

## 5. Conclusions and Prospects

Numerous studies in recent years have shown that LDH materials present strong synergistic effects. They have good effects not only in adsorbing inorganic pollutants but also in the photocatalysis of new organic pollutants. This will attract many scientists to conduct in-depth research on these materials. This article reviews the application of LDH-C as a synergistic material for adsorption, electrocatalysis, and photocatalysis and explains its mechanism of action. After a comprehensive analysis, it has been found that the material has not yet been analyzed enough in terms of the photocatalytic degradation experiment of new pollutants and needs more in-depth experimental studies by researchers, mainly in the following aspects:

- (1) The types of carbon materials that can be combined with LDHs lack diversity, especially in terms of biomass carbon materials. At present, there are many known types of biomass carbon materials but rare reports on biomass carbon materials that can produce composite LDHs on a large scale. In the future, research on the combination of biomass carbon and LDHs can be increased.
- (2) The mechanism analysis of the degradation of organic pollutants by LDH-C is not accurate enough. At present, the role of active radicals in the photocatalytic degradation reaction has been confirmed but the contribution of the carbon component in the composite material to the degradation of pollutants is still unclear and how the addition of carbon materials affects the transfer path or efficiency of photogenerated electrons is not detailed. In the future, the research on the mechanism of LDH-C degrading organic pollutants should be strengthened.
- (3) The application of research works on the LDH-C materials applied to practical wastewater treatment is not developed enough. It is necessary to transform the research from laboratory based to pilot plant and industrial-scale production and to study more parameters for the industrialization of such products.

Therefore, although the process of studying the characteristics of pollutants and the removal mechanism of LDH-C for pollutants has a long way to go, it is of great significance to develop high-efficiency and low-cost adsorbents and catalysts.

**Author Contributions:** Writing—original draft preparation, Y.H.; writing—review and editing, C.L., S.R., H.H., and L.Q. All authors have read and agreed to the published version of the manuscript.

**Funding:** This research was funded by the Science & Technology Program of Guangxi (Grant No.: Guike AD19110007, Guike AD19110105), Research Foundation of Guangxi Key Laboratory (Grant No.: Guikeneng 1801K010), and Research Foundation of Guilin University of Technology (Grant No.: GUTQDJJ201808).

**Institutional Review Board Statement:** Not applicable.

**Informed Consent Statement:** Not applicable.

**Data Availability Statement:** The data presented in this study are available upon request from the corresponding author.

**Conflicts of Interest:** The authors declare no conflict of interest.

## References

1. Jaishankar, M.; Tseten, T.; Anbalagan, N.; Mathew, B.B.; Beeregowda, K.N. Toxicity, mechanism and health effects of some heavy metals. *Interdiscip. Toxicol.* **2014**, *7*, 60–72. [[CrossRef](#)]
2. Ahmed, M.B.; Zhou, J.L.; Ngo, H.H.; Guo, W.; Chen, M. Progress in the preparation and application of modified biochar for improved contaminant removal from water and wastewater. *Bioresour. Technol.* **2016**, *214*, 836–851. [[CrossRef](#)] [[PubMed](#)]
3. Huang, S.; Ouyang, T.; Chen, J.; Wang, Z.; Liao, S.; Li, X.; Liu, Z.Q. Synthesis of nickel-iron layered double hydroxide via topochemical approach: Enhanced surface charge density for rapid hexavalent chromium removal. *J. Colloid Interface Sci.* **2022**, *605*, 602–612. [[CrossRef](#)] [[PubMed](#)]
4. Huo, J.; Min, X.; Dong, Q.; Xu, S.; Wang, Y. Comparison of Zn-Al and Mg-Al layered double hydroxides for adsorption of perfluorooctanoic acid. *Chemosphere* **2022**, *287*, 132297. [[CrossRef](#)]
5. Arif, M.; Liu, G.; Yousaf, B.; Ahmed, R.; Irshad, S.; Ashraf, A.; Zia-ur-Rehman, M.; Rashid, M.S. Synthesis, characteristics and mechanistic insight into the clays and clay minerals-biochar surface interactions for contaminants removal—A review. *J. Clean. Prod.* **2021**, *310*, 127548. [[CrossRef](#)]
6. Mochane, M.J.; Magagula, S.I.; Sefadi, J.S.; Sadiku, E.R.; Mokhena, T.C. Morphology, thermal stability, and flammability properties of polymer-layered double hydroxide (LDH) nanocomposites: A Review. *Crystals* **2020**, *10*, 612. [[CrossRef](#)]
7. Xie, Z.H.; Zhou, H.Y.; He, C.S.; Pan, Z.C.; Yao, G.; Lai, B. Synthesis, application and catalytic performance of layered double hydroxide based catalysts in advanced oxidation processes for wastewater decontamination: A review. *Chem. Eng. J.* **2021**, *414*, 128713. [[CrossRef](#)]
8. He, J.; Yang, Z.; Zhang, L.; Li, Y.; Pan, L. Cu supported on ZnAl-LDHs precursor prepared by in-situ synthesis method on  $\gamma$ -Al<sub>2</sub>O<sub>3</sub> as catalytic material with high catalytic activity for methanol steam reforming. *Int. J. Hydrog. Energy* **2017**, *42*, 9930–9937. [[CrossRef](#)]
9. Feng, X.; Yu, Z.; Long, R.; Li, X.; Shao, L.; Zeng, H.; Zeng, G.; Zuo, Y. Self-assembling 2D/2D (MXene/LDH) materials achieve ultra-high adsorption of heavy metals Ni<sup>2+</sup> through terminal group modification. *Sep. Purif. Technol.* **2020**, *253*, 117525. [[CrossRef](#)]
10. Olya, N.; Ghasemi, E.; Mahdavian, M.; Ramezanzadeh, B. Construction of a novel corrosion protective composite film based on a core-shell LDH-Mo@SiO<sub>2</sub> inhibitor nanocarrier with both self-healing/barrier functions. *J. Taiwan Inst. Chem. Eng.* **2020**, *113*, 406–418. [[CrossRef](#)]
11. Soheili-Azad, P.; Yaftian, M.R.; Dorraji, M.S.S. Application of zinc/aluminum layered double hydroxide nanosorbent in a fixed-bed column for SPE-preconcentration followed by HPLC determination of diclofenac in biological and hospital wastewater samples. *Microchem. J.* **2019**, *148*, 270–276. [[CrossRef](#)]
12. Lu, P.; Liu, Y.; Zhou, T.; Wang, Q.; Li, Y. Recent advances in layered double hydroxides (LDHs) as two-dimensional membrane materials for gas and liquid separations. *J. Membr. Sci.* **2018**, *567*, 89–103. [[CrossRef](#)]
13. Allou, N.B.; Saikia, J.; Bordoloi, P.; Yadav, A.; Pal, M.; Goswamee, R.L. Layered double hydroxide and microwave assisted functionalized carbon based nanocomposites as controlled release vehicle for antibiotics. *J. Drug Deliv. Sci. Technol.* **2019**, *49*, 243–253. [[CrossRef](#)]
14. Park, M.; Lee, C.I.; Lee, E.J.; Choy, J.H.; Kim, J.E.; Choi, J. Layered double hydroxides as potential solid base for beneficial remediation of endosulfan-contaminated soils. *J. Phys. Chem. Solids* **2004**, *65*, 513–516. [[CrossRef](#)]
15. Erickson, K.L.; Bostrom, T.E.; Frost, R.L. A study of structural memory effects in synthetic hydrotalcites using environmental SEM. *Mater. Lett.* **2005**, *59*, 226–229. [[CrossRef](#)]
16. Rosset, M.; F eris, L.A.; Perez-Lopez, O.W. Biogas dry reforming using Ni-Al-LDH catalysts reconstructed with Mg and Zn. *Int. J. Hydrog. Energy* **2021**, *46*, 20359–20376. [[CrossRef](#)]

17. Yang, W.; Kim, Y.; Liu, P.K.; Sahimi, M.; Tsotsis, T.T. A study by in situ techniques of the thermal evolution of the structure of a Mg–Al–CO<sub>3</sub> layered double hydroxide. *Chem. Eng. Sci.* **2002**, *57*, 2945–2953. [[CrossRef](#)]
18. Lv, Z.; Yang, S.; Zhu, H.; Chen, L.; Alharbi, N.S.; Wakeel, M.; Wahid, A.; Chen, C. Highly efficient removal of As(V) by using NiAl layered double oxide composites. *Appl. Surf. Sci.* **2018**, *448*, 599–608. [[CrossRef](#)]
19. Shen, J.C.; Zeng, H.Y.; Chen, C.R.; Xu, S. A facile fabrication of Ag<sub>2</sub>O-Ag/ZnAl-oxides with enhanced visible-light photocatalytic performance for tetracycline degradation. *Appl. Clay Sci.* **2020**, *185*, 105413. [[CrossRef](#)]
20. Chen, M.; Liu, J.; Bi, Y.; Rehman, S.; Dang, Z.; Wu, P. Multifunctional magnetic MgMn-oxide composite for efficient purification of Cd(2+) and paracetamol pollution: Synergetic effect and stability. *J. Hazard. Mater.* **2020**, *388*, 122078. [[CrossRef](#)]
21. Chen, M.; Wu, P.; Huang, Z.; Liu, J.; Li, Y.; Zhu, N.; Dang, Z.; Bi, Y. Environmental application of MgMn-layered double oxide for simultaneous efficient removal of tetracycline and Cd pollution: Performance and mechanism. *J. Environ. Manag.* **2019**, *246*, 164–173. [[CrossRef](#)] [[PubMed](#)]
22. Boumeriame, H.; Da Silva, E.S.; Cherevan, A.S.; Chafik, T.; Faria, J.L.; Eder, D. Layered double hydroxide (LDH)-based materials: A mini-review on strategies to improve the performance for photocatalytic water splitting. *J. Energy Chem.* **2022**, *64*, 406–431. [[CrossRef](#)]
23. He, S.; An, Z.; Wei, M.; Evans, D.G.; Duan, X. Layered double hydroxide-based catalysts: Nanostructure design and catalytic performance. *Chem. Commun.* **2013**, *49*, 5912–5920. [[CrossRef](#)]
24. Omwoma, S.; Chen, W.; Tsunashima, R.; Song, Y.F. Recent advances on polyoxometalates intercalated layered double hydroxides: From synthetic approaches to functional material applications. *Coord. Chem. Rev.* **2014**, *258–259*, 58–71. [[CrossRef](#)]
25. Guo, X.; Ruan, Y.; Diao, Z.; Shih, K.; Su, M.; Song, G.; Chen, D.; Wang, S.; Kong, L. Environmental-friendly preparation of Ni–Co layered double hydroxide (LDH) hierarchical nanoarrays for efficient removing uranium (VI). *J. Clean. Prod.* **2021**, *308*, 127384. [[CrossRef](#)]
26. Cosano, D.; Esquivel, D.; Romero, F.J.; Jiménez-Sanchidrián, C.; Ruiz, J.R. Microwave-assisted synthesis of hybrid organo-layered double hydroxides containing cholate and deoxycholate. *Mater. Chem. Phys.* **2019**, *225*, 28–33. [[CrossRef](#)]
27. Barahuie, F.; Hussein, M.Z.; Arulselvan, P.; Fakurazi, S.; Zainal, Z. Drug delivery system for an anticancer agent, chlorogenate-Zn/Al-layered double hydroxide nanohybrid synthesised using direct co-precipitation and ion exchange methods. *J. Solid State Chem.* **2014**, *217*, 31–41. [[CrossRef](#)]
28. Hu, J.; Zhao, G.; Long, X.; Wang, Y.; Jiao, F. In situ topotactic fabrication of ZnS nanosheet by using ZnAl- layered double hydroxide template for enhanced tetracycline pollutant degradation activity. *Mater. Sci. Semicond. Process.* **2021**, *134*, 106007. [[CrossRef](#)]
29. San Román, M.J.; Holgado, M.J.; Jaubertie, C.; Rives, V. Synthesis, characterisation and delamination behaviour of lactate-intercalated Mg,Al-hydroxalcite-like compounds. *Solid State Sci.* **2008**, *10*, 1333–1341. [[CrossRef](#)]
30. Okamoto, K.; Iyi, N.; Sasaki, T. Factors affecting the crystal size of the MgAl-LDH (layered double hydroxide) prepared by using ammonia-releasing reagents. *Appl. Clay Sci.* **2007**, *37*, 23–31. [[CrossRef](#)]
31. Qiu, X.; Wang, W. Removal of borate by layered double hydroxides prepared through microwave-hydrothermal method. *J. Water Process Eng.* **2017**, *17*, 271–276. [[CrossRef](#)]
32. Wang, J.; Wang, S. Preparation, modification and environmental application of biochar: A review. *J. Clean. Prod.* **2019**, *227*, 1002–1022. [[CrossRef](#)]
33. Yi, Y.; Huang, Z.; Lu, B.; Xian, J.; Tsang, E.P.; Cheng, W.; Fang, J.; Fang, Z. Magnetic biochar for environmental remediation: A review. *Bioresour. Technol.* **2020**, *298*, 122468. [[CrossRef](#)] [[PubMed](#)]
34. Li, Y.; Xing, B.; Ding, Y.; Han, X.; Wang, S. A critical review of the production and advanced utilization of biochar via selective pyrolysis of lignocellulosic biomass. *Bioresour. Technol.* **2020**, *312*, 123614. [[CrossRef](#)] [[PubMed](#)]
35. Liu, X.L. Non-covalent immobilization of C<sub>60</sub> in benzoic acid modified layered double hydroxides. *Asian J. Chem.* **2013**, *25*, 4703–4704. [[CrossRef](#)]
36. Lestari, P.R.; Takei, T.; Kumada, N. Novel ZnTi/C<sub>3</sub>N<sub>4</sub>/Ag LDH heterojunction composite for efficient photocatalytic phenol degradation. *J. Solid State Chem.* **2021**, *294*, 121858. [[CrossRef](#)]
37. Li, M.; Zhu, J.E.; Zhang, L.; Chen, X.; Zhang, H.; Zhang, F.; Xu, S.; Evans, D.G. Facile synthesis of NiAl-layered double hydroxide/graphene hybrid with enhanced electrochemical properties for detection of dopamine. *Nanoscale* **2011**, *3*, 4240–4246. [[CrossRef](#)]
38. Wang, T.; Zhang, D.; Fang, K.; Zhu, W.; Peng, Q.; Xie, Z. Enhanced nitrate removal by physical activation and Mg/Al layered double hydroxide modified biochar derived from wood waste: Adsorption characteristics and mechanisms. *J. Environ. Chem. Eng.* **2021**, *9*, 105184. [[CrossRef](#)]
39. Hu, F.; Wang, M.; Peng, X.; Qiu, F.; Zhang, T.; Dai, H.; Liu, Z.; Cao, Z. High-efficient adsorption of phosphates from water by hierarchical CuAl/biomass carbon fiber layered double hydroxide. *Colloids Surf. A* **2018**, *555*, 314–323. [[CrossRef](#)]
40. Amin, M.T.; Alazba, A.A.; Shafiq, M. LDH of NiZnFe and its composites with carbon nanotubes and date-palm biochar with efficient adsorption capacity for RB5 dye from aqueous solutions: Isotherm, kinetic, and thermodynamics studies. *Curr. Appl. Phys.* **2020**, in press. [[CrossRef](#)]
41. Wang, T.; Li, C.; Wang, C.; Wang, H. Biochar/MnAl-LDH composites for Cu (II) removal from aqueous solution. *Colloids Surf. A* **2018**, *538*, 443–450. [[CrossRef](#)]

42. Baruah, A.; Mondal, S.; Sahoo, L.; Gautam, U.K. Ni-Fe-layered double hydroxide/N-doped graphene oxide nanocomposite for the highly efficient removal of Pb(II) and Cd(II) ions from water. *J. Solid State Chem.* **2019**, *280*, 120963. [[CrossRef](#)]
43. Cheng, X.; Deng, J.; Li, X.; Wei, X.; Shao, Y.; Zhao, Y. Layered double hydroxides loaded sludge biochar composite for adsorptive removal of benzotriazole and Pb(II) from aqueous solution. *Chemosphere* **2021**, *287*, 131966. [[CrossRef](#)] [[PubMed](#)]
44. Wu, Y.; Wang, H.; Sun, Y.; Xiao, T.; Tu, W.; Yuan, X.; Zeng, G.; Li, S.; Chew, J.W. Photogenerated charge transfer via interfacial internal electric field for significantly improved photocatalysis in direct Z-scheme oxygen-doped carbon nitrogen/CoAl-layered double hydroxide heterojunction. *Appl. Catal. B* **2018**, *227*, 530–540. [[CrossRef](#)]
45. Ju, L.; Wu, P.; Yang, L. Synthesis of ZnAlTi-LDO supported C<sub>60</sub>@AgCl nanoparticles and their photocatalytic activity for photo-degradation of bisphenol A. *Appl. Catal. B* **2018**, *224*, 159–174. [[CrossRef](#)]
46. Mureseanu, M.; Radu, T.; Andrei, R.D.; Darie, M.; Carja, G. Green synthesis of g-C<sub>3</sub>N<sub>4</sub>/CuONP/LDH composites and derived g-C<sub>3</sub>N<sub>4</sub>/MMO and their photocatalytic performance for phenol reduction from aqueous solutions. *Appl. Clay Sci.* **2017**, *141*, 1–12. [[CrossRef](#)]
47. Jo, W.K.; Tonda, S. Novel CoAl-LDH/g-C<sub>3</sub>N<sub>4</sub>/RGO ternary heterojunction with notable 2D/2D/2D configuration for highly efficient visible-light-induced photocatalytic elimination of dye and antibiotic pollutants. *J. Hazard. Mater.* **2019**, *368*, 778–787. [[CrossRef](#)]
48. Wang, P.; Ng, D.H.L.; Zhou, M.; Li, J. Freely standing MgAl-layered double hydroxides nanosheets and their derived metal oxides on g-C<sub>3</sub>N<sub>4</sub> thin-layer designed for obtaining synergic effect of adsorption and photocatalysis. *Appl. Clay Sci.* **2019**, *178*, 105131. [[CrossRef](#)]
49. Yu, Y.; Chen, D.; Xu, W.; Fang, J.; Sun, J.; Liu, Z.; Chen, Y.; Liang, Y.; Fang, Z. Synergistic adsorption-photocatalytic degradation of different antibiotics in seawater by a porous g-C<sub>3</sub>N<sub>4</sub>/calcined-LDH and its application in synthetic mariculture wastewater. *J. Hazard. Mater.* **2021**, *416*, 126183. [[CrossRef](#)]
50. Azalok, K.A.; Oladipo, A.A.; Gazi, M. UV-light-induced photocatalytic performance of reusable MnFe-LDO–biochar for tetracycline removal in water. *J. Photochem. Photobiol. A* **2021**, *405*, 112976. [[CrossRef](#)]
51. Yang, X.; Gao, Y.; Zhao, Z.; Tian, Y.; Kong, X.; Lei, X.; Zhang, F. Three-dimensional spherical composite of layered double hydroxides/carbon nanotube for ethanol electrocatalysis. *Appl. Clay Sci.* **2021**, *202*, 105964. [[CrossRef](#)]
52. Feng, Y.; Wang, X.; Huang, J.; Dong, P.; Ji, J.; Li, J.; Cao, L.; Feng, L.; Jin, P.; Wang, C. Decorating CoNi layered double hydroxides nanosheet arrays with fullerene quantum dot anchored on Ni foam for efficient electrocatalytic water splitting and urea electrolysis. *Chem. Eng. J.* **2020**, *390*, 124525. [[CrossRef](#)]
53. Dinari, M.; Allami, H.; Momeni, M.M. A high-performance electrode based on Ce-doped nickel-cobalt layered double hydroxide growth on carbon nanotubes for efficient oxygen evolution. *J. Electroanal. Chem.* **2020**, *877*, 114643. [[CrossRef](#)]
54. Kumar, O.P.; Ashiq, M.N.; Shah, S.S.A.; Akhtar, S.; Al-Obaidi, M.A.; Mujtaba, I.M.; Rehman, A.U. Nanoscale ZrRGO/CuFe layered double hydroxide composites for enhanced photocatalytic degradation of dye contaminant. *Mater. Sci. Semicond. Process.* **2021**, *128*, 105748. [[CrossRef](#)]
55. Yekan Motlagh, P.; Khataee, A.; Sadeghi Rad, T.; Hassani, A.; Joo, S.W. Fabrication of ZnFe-layered double hydroxides with graphene oxide for efficient visible light photocatalytic performance. *J. Taiwan Inst. Chem. E* **2019**, *101*, 186–203. [[CrossRef](#)]
56. Ou, B.; Wang, J.; Wu, Y.; Zhao, S.; Wang, Z. Efficient removal of Cr(VI) by magnetic and recyclable calcined CoFe-LDH/g-C<sub>3</sub>N<sub>4</sub> via the synergy of adsorption and photocatalysis under visible light. *Chem. Eng. J.* **2020**, *380*, 122600. [[CrossRef](#)]
57. Zheng, Z.; Ali, A.; Su, J.; Fan, Y.; Zhang, S. Layered double hydroxide modified biochar combined with sodium alginate: A powerful biomaterial for enhancing bioreactor performance to remove nitrate. *Bioresour. Technol.* **2021**, *323*, 124630. [[CrossRef](#)]
58. Laipan, M.; Zhu, J.; Xu, Y.; Sun, L.; Zhu, R. Fabrication of layered double hydroxide/carbon nanomaterial for heavy metals removal. *Appl. Clay Sci.* **2020**, *199*, 105867. [[CrossRef](#)]
59. Huang, Q.; Chen, Y.; Yu, H.; Yan, L.; Zhang, J.; Wang, B.; Du, B.; Xing, L. Magnetic graphene oxide/MgAl-layered double hydroxide nanocomposite: One-pot solvothermal synthesis, adsorption performance and mechanisms for Pb<sup>2+</sup>, Cd<sup>2+</sup>, and Cu<sup>2+</sup>. *Chem. Eng. J.* **2018**, *341*, 1–9. [[CrossRef](#)]
60. Lyu, P.; Wang, G.; Wang, B.; Yin, Q.; Li, Y.; Deng, N. Adsorption and interaction mechanism of uranium(VI) from aqueous solutions on phosphate-impregnation biochar cross-linked Mg–Al layered double-hydroxide composite. *Appl. Clay Sci.* **2021**, *209*, 106146. [[CrossRef](#)]
61. Sun, Q.; Chen, B. Biotemplated fabrication of 3D hierarchically porous MgAl-LDH/CF composites with effective adsorption of organic dyes from wastewater. *Ind. Eng. Chem. Res.* **2020**, *59*, 16838–16850. [[CrossRef](#)]
62. Sirajudheen, P.; Karthikeyan, P.; Meenakshi, S. Mechanistic performance of organic pollutants removal from water using Zn/Al layered double hydroxides imprinted carbon composite. *Surf. Interfaces* **2020**, *20*, 100581. [[CrossRef](#)]
63. Nayak, S.; Mohapatra, L.; Parida, K. Visible light-driven novel g-C<sub>3</sub>N<sub>4</sub>/NiFe-LDH composite photocatalyst with enhanced photocatalytic activity towards water oxidation and reduction reaction. *J. Mater. Chem. A* **2015**, *36*, 18622–18635. [[CrossRef](#)]
64. Liu, J.; Li, J.; Bing, X.; Ng, D.H.L.; Cui, X.; Ji, F.; Kionga, D.D. ZnCr-LDH/N-doped graphitic carbon-incorporated g-C<sub>3</sub>N<sub>4</sub> 2D/2D nanosheet heterojunction with enhanced charge transfer for photocatalysis. *Mater. Res. Bull.* **2018**, *102*, 379–390. [[CrossRef](#)]